A Cyclic Nonlinear Macro Model for Numerical Simulation of Beam-Column Joints in Existing Concrete Buildings

Wael M. Hassan
Skidmore, Owings & Merrill LLP, San Francisco, CA, USA
Jack P. Moehle
University of California, Berkeley, CA, USA

15 WCEE
LISBOA 2012

ABSTRACT
Earthquake reconnaissance has reported the substantial damage that can result from inadequate reinforced concrete beam-column joints. In some cases, failure of older-type corner joints appears to have led to building collapse. Models for joints with ductile details are widely available. Fewer models exist for joints that lack transverse reinforcement (unconfined joints), a common deficiency in buildings constructed prior to developing details for ductility in the 1970s.

This paper presents analytical tools for nonlinear modeling of exterior and corner joints in existing concrete buildings. A new nonlinear macro model is developed to model cyclic performance. The model incorporates new expressions for joint shear strength and axial capacity. In addition, the effects of axial load level, joint aspect ratio, and mode of joint failure on the constitutive cyclic backbone of unconfined joints are considered. Cyclic strength and stiffness degradation, pinching parameters, and bond-slip expressions are suggested. The model successfully models test cyclic performance of unconfined exterior and corner joints and offers an alternative means to the existing recommendations of nonlinear modeling of unconfined joints, which proved to be conservative.

Keywords: Shear strength, transverse reinforcement, seismic, assessment, concrete frame

1. MODELING JOINT BEHAVIOR FOR NUMERICAL SIMULATION

1.2. Conventional Rigid Joint Model

A common engineering practice has been to model the beam-column joints in concrete frames as rigid elements spanning the full joint dimensions. Some analysts have recognized that this model overestimates stiffness and instead have used a model in which the beam and column flexibilities extend to the joint centerline. Studies show that the rigid joint model overestimates stiffness and underestimates drift because of ignoring join shear deformations and slip of reinforcement. The centerline model can overestimate or underestimate stiffness. Rigid joint stiffness overestimation shortens natural period and affects the attracted seismic forces. Recent tests (Hassan 2011) showed that joint flexibility contributed significantly, up to 40%, to overall drift, especially in the nonlinear range.

1.3. ASCE/SEI 41-06 Nonlinear Joint Model

ASCE/SEI 41-06 suggests modeling joints in concrete frame linear analysis using rigid links that cover partially or fully the joint dimensions. The modeling approach accounts for beam bar slip rotation using reduced flexural column and beam stiffness. For nonlinear analysis, ASCE 41 suggests a backbone curve for joint shear strain modeling, with shear strength based on the number of members framing into the joint. However, approaches to implement this model are not described. Figure 1.1 shows joint shear stress-strain backbone relations from tests compared to the nonlinear joint model backbones of ASCE 41 for specimens U-J-2 and U-J-1 tested by Hassan 2010. It is clear that ASCE 41 is quite conservative in terms of estimating joint shear strength and plastic shear deformations. These backbone curves will be implemented in a cyclic model for comparison with cyclic test data in a subsequent section.

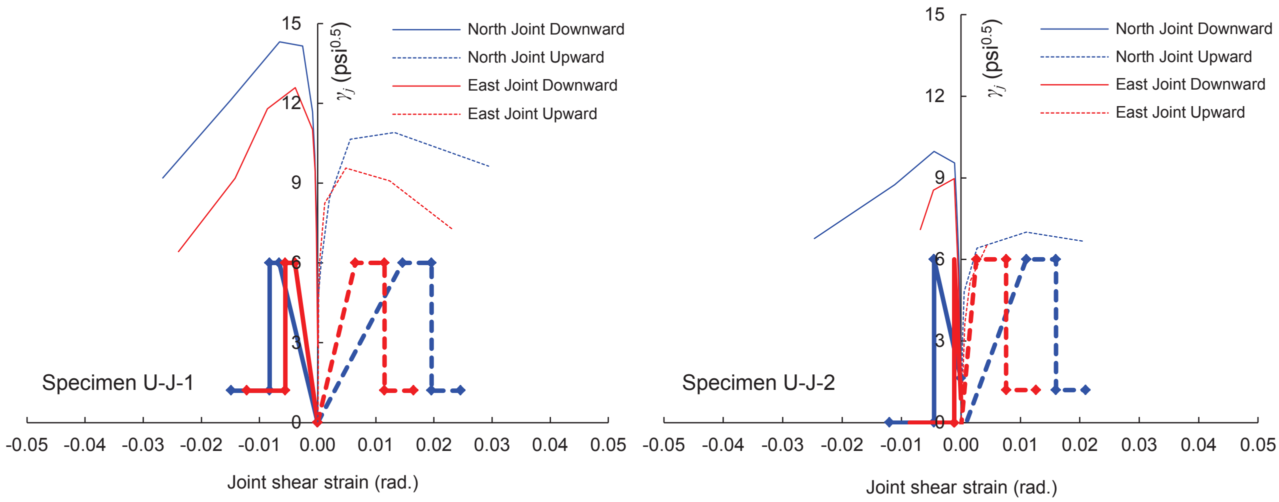

Figure 1.1. Joint nonlinear models (lines with diamonds refer to ASCE 41, plain lines refer to tests by Hassan 2011)

1.3. Rotational Spring with Rigid Links Joint Model (Scissors Model)

Many nonlinear joint models are available. Hassan 2011 summarizes the available macro models for joint simulation.. However, some of these models may be unsuitable for older concrete building assessment, either because they were developed and calibrated for confined joints or because they are complicated to use. One of the models that may be suitable, designated the scissors model, is a relatively simple model composed of a rotational spring with rigid links that span the joint dimensions. This model is a simplification of macro model developed originally for steel panel zones. The model was first suggested by Alath and Kunnath, 1995. The model was also tested by Celik and Ellingwood, 2008 and showed promising results. This study extends this model for unconfined exterior and corner joints under high axial compression and tension loads.

2. PROPOSED JOINT MACRO MODEL

The proposed exterior and corner joint macro model adopts the scissors concept (Fig. 2.1). The element is implemented through defining duplicate master and slave nodes at the center of the joint connected with a zero length rotational spring. The degrees of freedom at the two central nodes are defined to permit only relative rotation through the constitutive model of the rotational spring, thereby representing shear deformation of the joint.

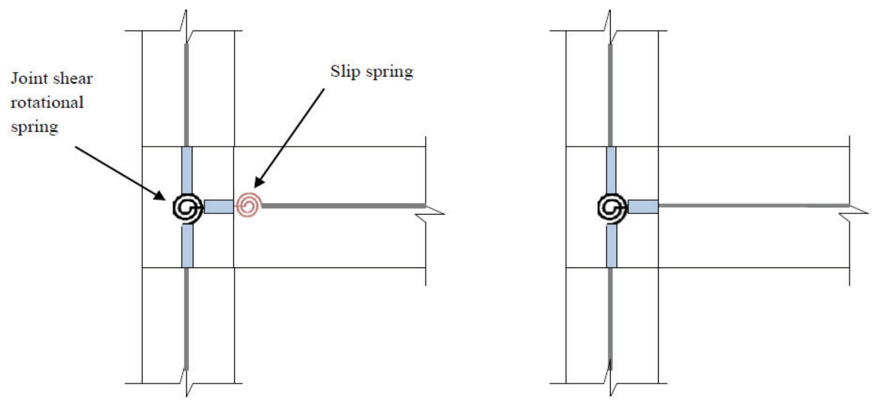

Figure 2.1. Proposed scissors model: (a) Explicit slip modeling, (b) Implicit slip modeling

2.1 Proposed Shear Stress-Strain Backbone Curves

The constitutive material model of the rotational spring element is defined through the joint shear stress-strain backbone curve presented in Fig. 2.2 and Table 1. The multi-linear backbone curve was calibrated using results from 12 unconfined joint tests by Hassan, 2011, Park, 2010, and Pantelides, et al., 2002.The moment transferred through the rotational spring M_j is related to the joint shear stress τ_j through:

$$M_j = \tau_j A_j \frac{L}{\frac{L - h_c/2}{jd_b} - \frac{L}{H}} \tag{2.1}$$

where L is the length from beam inflection point to the column centerline, approximated as half beam centerline span, d_b is the effective beam depth, A_j is the effective joint area according to ACI 352-02. The parameter j is the effective beam lever arm ratio, which can be approximated as 0.90. The current model accounts for J-Failure, and for BJ-Failure with high axial load ratio. The column height H is measured between column inflection points, approximated as the story height. The rotation of the spring can be defined in two ways. One way is to consider the joint panel rotation as solely the joint shear strain:

$$\theta_j = \gamma_s \tag{2.2}$$

In this case, the joint rotation resulting from beam bar slip is explicitly defined by a separate zero length rotational slip spring attached between the beam-joint interface section and the end of the beam rigid link as shown in Fig. 2.1.a. The other assumption, Fig. 2.1.b, is to include the joint rotation due to average beam and column bar slip θ_{slip} by adding it to the joint shear strain as:

$$\theta_j = \gamma_s + \theta_{slip} \tag{2.3}$$

In this case there will be no need for a separate slip spring for the beam. This latter approach imposes the same slip rotation on the beam and the column. Hassan 2011 shows that both slip modeling options yield similar responses with no major advantage for one option over the other. Equations 2.1 through 2.3 can be used to switch between joint shear stress-strain/rotation constitutive model and moment-rotation constitutive models. The proposed backbone curve characteristic points are presented in Table 1 and discussed next.

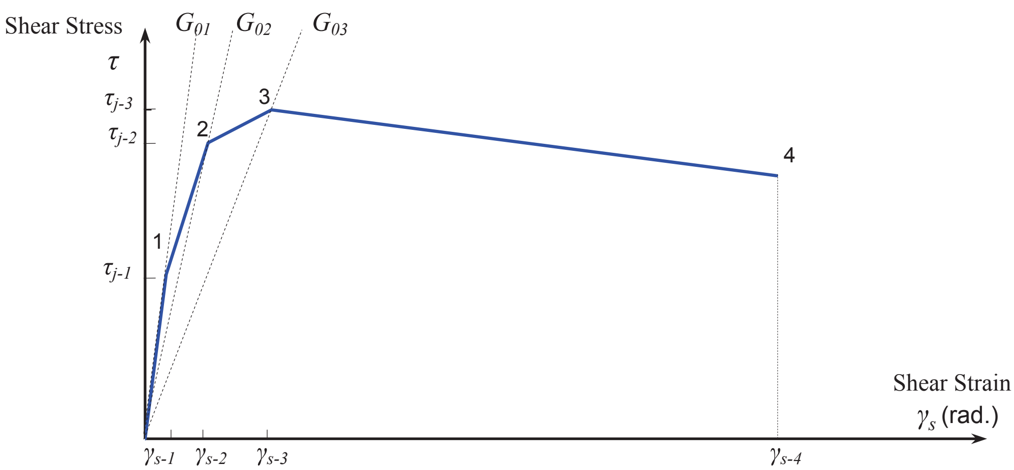

Figure 2.2. Proposed shear stress-strain backbone curve for joint rotational spring model

2.1.1. Point 1: Cracking Strength

This point represents the hairline joint cracking limit state. In the modified compression field theory, the cracking shear strain of a plain concrete shear panel is 0.00012, invariantly in unconfined and confined joints. However, observed unconfined beam-column joint test cracking shear strains range from 0.0001 to 0.0013. Apparently, the state of stress in beam-column joints does not resemble that in plain shear panels. Here we adopted the approach of Uzumeri 1977 (see Table 1). The initial joint shear modulus of rigidity G_{01} was found to be 50% the theoretical elastic shear modulus of concrete: G_c, which is $5E_c/(1+v)$, where v=0.20 is concrete Poisson's ratio, and E_c is the concrete modulus of elasticity.

Table 1. Joint Macro Model Constitutive Relationships

	Point 1: Cracking		Point 2: Yield (Pre-Peak)	
	Downward and upward		Downward	Upward
Shear Stress	$\frac{\tau_{j-1}}{\sqrt{f_c^{'}}} = 3.5\sqrt{1+0.002\frac{P}{A_j}} \le 0.6\frac{\tau_{j-3}}{\sqrt{f_c^{'}}}$		$\tau_{j-2} = \gamma_{s-2}G_{02} \ge 0.9\tau_{j-3}$ $\tau_{j-2} = 0.9\tau_{j-3}^{\#}$	$\tau_{j-2} = \gamma_{s-2}G_{02} \ge 0.9\tau_{j-3}$ $\tau_{j-2} = 0.9\tau_{j-3}^{\#}$
Shear Strain	$\gamma_{s-1} = \frac{\tau_{j-1}}{G_{01}}$		$\gamma_{s-2} = 0.002$ $\gamma_{s-2} = 0.0002^{\#}$	$\gamma_{s-2} = 0.0025$ $\gamma_{s-1} = \frac{\tau_{j-2}}{G_{02}}^{\#}$
Shear Modulus	$G_{01} = 0.5G_c$		$G_{02} = 0.1G_c$	$G_{02} = 0.1G_c$
	Point 3 (Peak Shear Strength)		Point 4 (Axial Failure)	
	Downward	Upward	Downward	Upward
Shear Stress	$\tau_{j-3} = V_j / A_j$ $\tau_{j-3} = 1.1\tau_{j-2}^{\#}$	$\tau_{j-3} = \gamma_3\sqrt{f_c^{'}}$ $\tau_{j-3} = 1.1\tau_{j-2}^{\#}$	$\tau_{j-4} = 0.7\tau_{j-3}$	$\tau_{j-4} = 0.8\tau_{j-3}$
Shear Strain	$\gamma_{s-3} = \frac{\tau_{j-3}}{G_{03}}$ $\gamma_{s-3} = 0.0002^{\#}$	$\gamma_{s-3} = \frac{\tau_{j-3}}{G_{03}}$	For $\frac{P}{f_c^{'}A_j} > 0.3$ $\gamma_{s-4} = \gamma_{s-3} + 0.02$ For $\frac{P}{f_c^{'}A_j} \le 0.3$ $\gamma_{s-4} = \gamma_{s-3} + 0.025$	$\gamma_{s-4} = 0.03$
Shear Modulus	For $\frac{P}{f_c^{'}A_j} \ge 0.3$ $G_{03} = \left(0.14 - \frac{3}{80}\alpha_j\right)G_c$ For $\frac{P}{f_c^{'}A_j} < 0.3$ $G_{03} = \left(0.175 - \frac{3}{40}\alpha_j\right)G_c$	$G_{03} = 0.03G_c$ $G_{03} = 0.02G_c^{\#}$	NA	NA

BJ-Failure mode expressions with axial load ratio higher than 0.3

2.1.2. Point 2: Pre-Peak "Yielding" Strength

For J-Failure mode, the limit state damage level reflected by point 2 is denoted "pre-peak" level. At this level, main diagonal crack is widened and additional secondary diagonal cracks develop. For BJ-Failure mode, the limit state that point 2 represents is the yielding of the beam. The secant joint shear modulus at point 2, G_{02}, and the shear strain at this point are given by in Table 1. For BJ failure mode downward loading under axial load higher than $0.3f_c^{'}A_j$ the joint shear strains corresponding to points 1, 2, and 3 are negligible. A fitted lower bound of 90% of the peak joint shear stress is set for the shear stress at point 2.

2.1.3 Point 3: Peak Shear Strength

The peak shear strength of J-failure joints can be obtained from joint shear strength coefficient using the strut-and-tie model proposed in Hassan et al., 2010 or the following empirical shear strength model:

$$V_j = 11.25\alpha_j^{-0.50}\kappa A_j\sqrt{f_c^{'}} \qquad \text{(lb., inch units)} \tag{2.4}$$

α_j is the joint aspect ratio h_b/h_c (beam to column depth ratio) and κ is the axial load enhancement factor:

$$\kappa = 1+(0.86-0.31\alpha_j)\left[\frac{P}{f_c^{'}A_g}-0.15\right] \qquad 1\le\kappa\le 1.35-0.10\alpha_j \tag{2.5}$$

Table 1 presents the remaining modeling parameters for point 3. For the BJ-Failure mode, the joint shear stress $\tau_{j\text{-}2}$ corresponding to beam strain-hardening capacity can be used to calculate the shear stress at point 3. This can be approximated as 1.1 times the joint shear stress coefficient corresponding to actual beam yield or 1.25 times that corresponding to nominal flexural capacity.

2.1.4 Point 4: Post-Peak (Residual /Axial Failure) Strength

The post-peak strength can be expressed as the residual shear strength corresponding to the maximum drift reached prior to axial failure in the case of high axial load (larger than $0.3f_c^{'}A_j$) or to very large shear deformations and severe joint distress that correspond to large story drifts in the case of axial loads below $0.3f_c^{'}A_j$. Based on the test results in Hassan 2010, a shear stress of 70% the peak joint shear strength was found to be representative in both cases. To continue the analysis until reaching actual axial failure, it is recommended to extend the line connecting points 3 and 4 of the backbone curve to terminate the analysis at 50% peak shear stress. It is emphasized here that the shear stress and "strain" given by Table 1 correspond to a point immediately prior to axial failure of the joint or to a very large drift of the building. The drift capacity at axial failure $(\Delta/L)_{axial}$ of a shear damaged joint can be estimated using bottom beam reinforcement A_{sb} and yield strength f_{yb} along with shear crack angle θ, calculated according to Hassan 2011 as:

$$\left(\frac{\Delta}{L}\right)_{axial} = 0.057\left(\frac{P.\tan\theta}{A_{sb}f_{yb}}\right)^{-0.5} \tag{2.6}$$

2.2. Joint Rotational Spring Hysteretic Material Model

The one dimensional material model used to implement the proposed backbone curve for the joint constitutive model and to describe the hysteresis, pinching, energy dissipation, and cyclic degradation of the response is the *Pinching4* material model in OpenSees, by Lowes and Altoontash 2003. This model is particularly useful to represent the pinched hysteretic behavior of shear critical elements such as unconfined joints. Model parameters suitable for unconfined joints are defined in Hassan 2011. The model has different parameters for pinching behavior, unloading and reloading stiffness degradation, strength degradation, and energy dissipation. The 22 parameters were calibrated for the proposed backbone curves in this paper.

2.3. Bond-Slip Modeling

There are several techniques to represent bond-slip rotation in an analytical model of a beam-column joint. The most direct approach is to introduce a slip spring whose properties are either calibrated directly from tests or calculated using a bond-slip model. An alternative is to scale the moment-shear strain (rotation) backbone to account for higher rotation resulting from slip; this method was used successfully by Celik and Ellingwood, 2008. Yet another approach is to reduce the effective stiffness of beams and columns to account for slip deformation as recommended by ASCE 41. In the present study, the first approach is used with an explicit slip spring, Fig. 2.1.b, whose details of bond-slip model are described in Hassan 2011. The uniaxial *Hysteretic Material* in OpenSees framework has been used.

3. SIMULATION OF BEAM-COLUMN JOINT SUB-ASSEMBLAGES

3.1. Model Geometry

The finite element model geometry used to simulate the test beam-column joint sub-assemblage is shown in Fig. 3.1. Simulations were conducted for test specimens U-J-1, U-J-2, U-BJ-1 of Hassan, 2011, and SP4 of Park, 2010. For model validation, further simulation studies were performed on specimens BS-L and BS-L-600, Wong, 2005, that were not used to calibrate the model. The subassebmlages with actual test boundary conditions were modeled in OpenSees 2.2.2 platform.

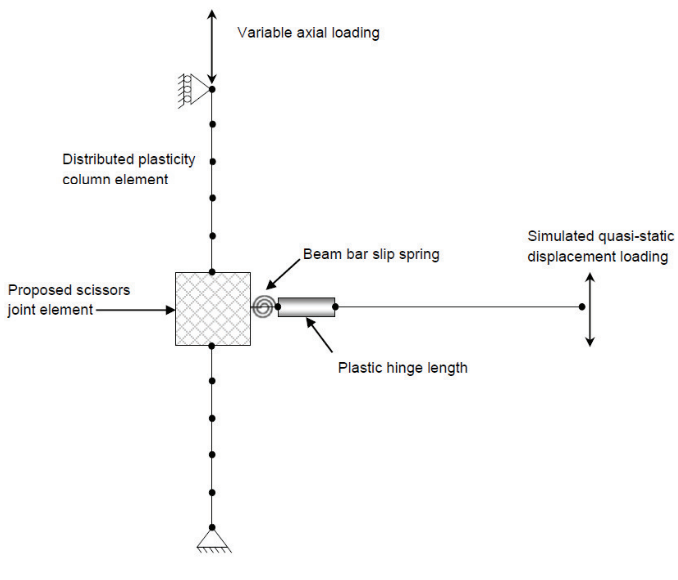

Figure 3.1. Hassan 2011 beam-column joint test simulation model

3.2. Material and Components Simulation Models

Uniaxial stress-strain concrete and steel materials were used to model the specimens at the section level. *Concrete02* material with uniaxial tension and compression was used to model concrete behavior. The model features linear tension softening to represent inelastic tension action. The unconfined cover concrete parameters and the maximum tensile stress were obtained from test date cylinders.. Since significant ductility enhancement is provided by confinement, a modification to the *Concrete02* unconfined properties was used to account for this enhancement according to the model of Kent and Park 1971. *Steel02* material model was used to model the uniaxial cyclic behavior of reinforcing steel. The model uses a bilinear backbone, and the Menegotto-Pinto model for loading and unloading rules. Monotonic steel properties are based on reported materials tests. The column section was discretized as fiber section with one-dimensional steel and concrete material models to model axial load-moment interaction. The columns were modeled on the member level with distributed inelasticity model with four integration points along the column height. A fiber section is used along the column height to account for effects of axial load variation due to overturning. Beam sections were discretized as fiber sections. Reinforcing steel bars were modeled in the section using the as-built effective depth reported by authors. The beams were modeled using *beamWithHinges2* element, which is a force-based elastic element along the beam length with all inelasticity concentrated at the beam ends. The advantage of this element is that there are two inelastic fiber sections spaced apart by the plastic hinge length at each beam end, which resembles the physical plastic hinge region length. A plastic hinge length $0.5h_b$ was used.

4. NUMERICAL SIMULATION RESULTS AND MODEL VALIDATION

4.1 Proposed Joint Macro Model Simulation Results

Figures 4.1 and 4.2 show the simulation results using the proposed scissors joint model combined with an explicit bond-slip spring for specimens U-J-2, U-J-1 and U-BJ-1. The proposed model was able to simulate the response of specimen U-J-2 when the joint is subjected to compressive axial load successfully. However, it slightly overestimated the initial stiffness of the specimen when the overturning moment brings the joint into tension or small compression. The model slightly underestimates the drift at peak shear strength. It is worth mentioning that the model does not properly represent the response of the last downward loading cycle that triggered axial failure (second cycle at -3.42% drift). As seen in Fig. 4.2, the proposed joint scissors model simulated the cyclic response of specimen U-J-1 with reasonable accuracy. Similar to specimen U-J-2, the model slightly underestimated the drift at peak shear strength drift in the downward loading direction. The simulated response in the upward loading direction was less accurate than that in the downward loading direction in terms of strength degradation envelope. This might be attributed to the calibration procedure followed for the proposed model, which did not account for the degrading axial tension force that took place during specimen U-J-1 testing. As seen in Fig. 4.2, the proposed model was able to successfully simulate the response of the specimen U-BJ-1 with slight underestimation of pinching in the tension cycles. Results for specimen SP4 also show good correlation (Figure 4.3).

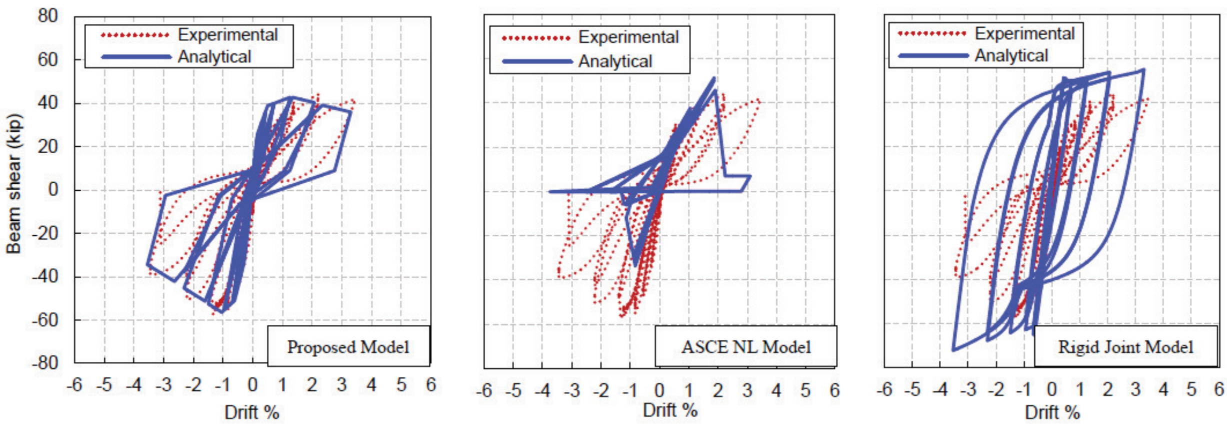

Figure 4.1. Simulation results of specimen U-J-2, Hassan 2011

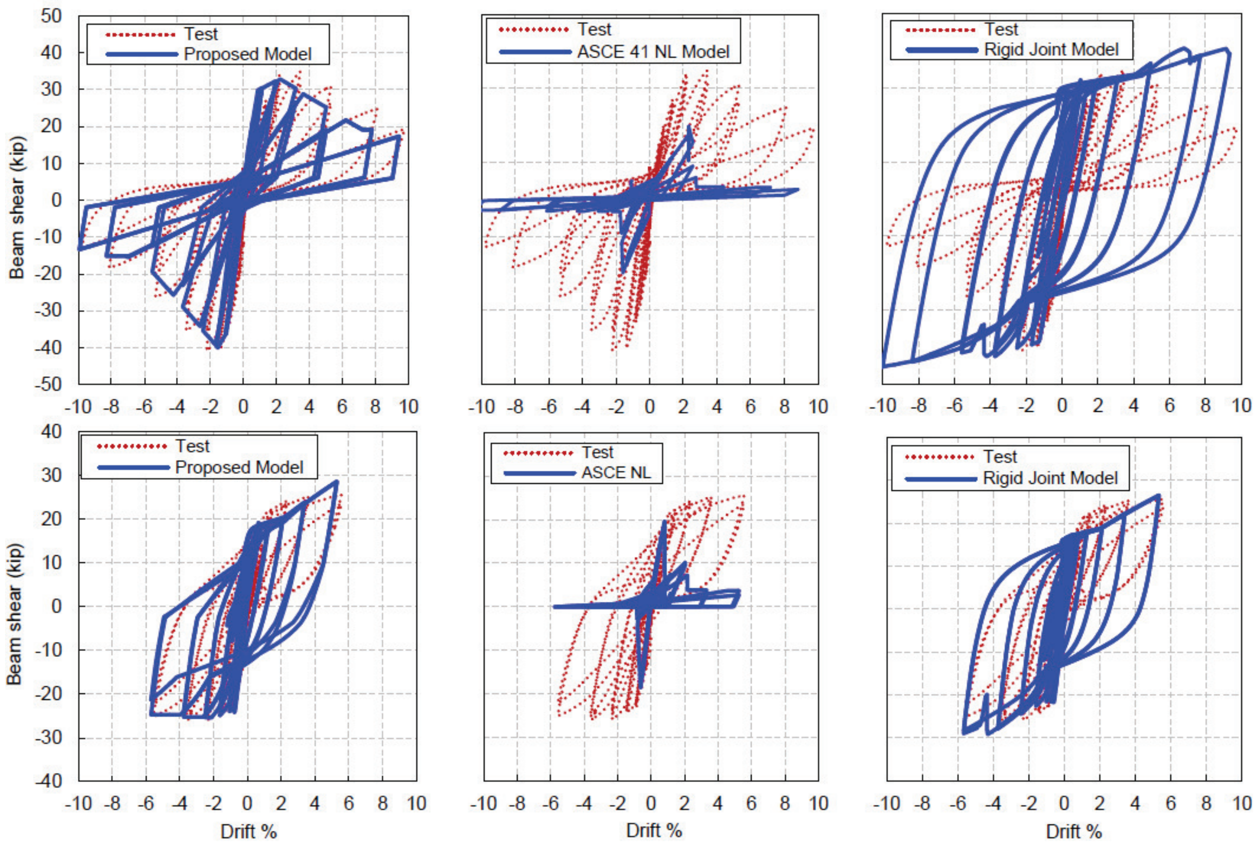

Figure 4.2. Simulation results of specimens U-J-1 (top) and U-BJ-1 (bottom), Hassan 2011

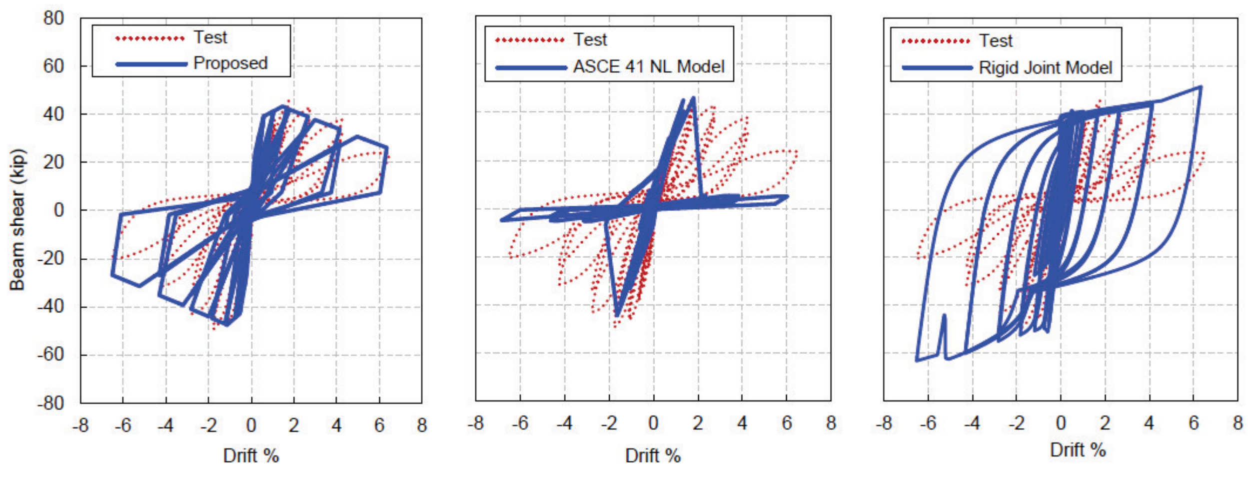

Figure 4.3. Simulation results of Park 2010 specimen SP4

4.2 Rigid Joint Model Simulation Results

Specimens U-J-1, U-J-2, and SP4 sustained J-Failure modes. Figures 4.1 through 4.3 show the force-drift simulation responses for those specimens using the conventional rigid joint assumption. The simulated response of all three specimens is dominated by beam flexural capacity. These deviate unacceptably from the measured behavior. Figure 4.2 shows the force-drift simulation response for specimen U-BJ-1, which experienced BJ-Failure during the test, using the rigid joint model. The simulation in this case is reasonably good, although the force-deformation response shows wider hysteresis than observed in the test.

4.3. Simulation Response using ASCE 41 Nonlinear Modeling Provisions

Figures 4.1 through 4.3 show the force-drift simulation response for specimen U-J-1 and U-J-2, and SP4 using the ASCE 41 strength and nonlinear joint modeling provisions. The results indicate that the ASCE 41 model can produce unacceptably inaccurate response. Post-peak plastic deformations were significantly underestimated. The calculated steep strength loss immediately following the peak joint shear strength does not resemble the test results. In addition, the peak shear strength coefficient suggested by ASCE 41 significantly underestimates the actual strength.

4.4. Model Validation and Calibration

To further investigate the appropriateness of the proposed joint model for unconfined exterior and corner joints, five additional joint tests, not used for model calibration, were simulated using the proposed model. Results for only three are presented here owing to space limitations. Of these, BS-L, BS-L600 (Wong 2005) sustained J-Failure modes while specimen SP2 (Park 2010) sustained slight beam yielding prior to reaching peak joint shear strength. In general, the proposed model was able to simulate the test response with reasonable accuracy (Figure 4.4).The model simulation for specimen BS-L-600 was symmetric for both loading directions due to symmetric beam reinforcement. The test response, however, was unsymmetrical for reasons not fully understood. The proposed model simulated the response of specimen SP2 with good accuracy. After initial beam yielding, the simulated strength degradation was controlled by the joint degradation envelope. This is consistent with test observations of specimen SP2.

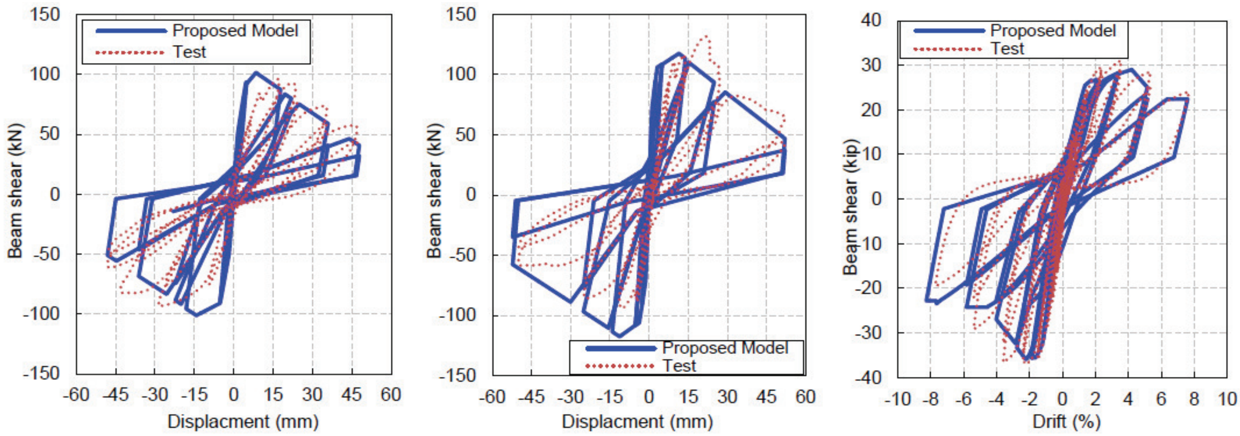

Figure 4.4. Proposed joint model simulation of specimens BS-L and BS-L600 (Wong 2005), and SP2 (Park 2010)

5. CONCLUSIONS

1. Rigid joint modeling for unconfined joints in concrete frames can lead to grossly inaccurate simulations of beam-column joint response, especially in cases where joint failure is a controlling mechanism. For joints with BJ-Failure mode, the rigid joint model resembled test cyclic response more reasonably. This is because the response in BJ-Failure mode initially is dominated by beam yielding with a high joint rigidity.
2. The shear strength provisions of ASCE 41 are inaccurate for unconfined exterior and corner joints because they do not account for several parameters that may affect joint strength, including joint aspect ratio, beam reinforcement ratio, axial load ratio, and bidirectional loading. The ASCE 41 nonlinear modeling parameters for unconfined joints are overly conservative, especially with high axial loads, resulting in unrealistically severe strength degradation and low drift capacity.

3. A cyclic constitutive model backbone curve was proposed for nonlinear modeling of shear parameters of unconfined exterior and corner beam-column joints in finite element building simulation. The model incorporates the effect of axial load level, joint aspect ratio, joint failure mode, and axial capacity.
4. The proposed rotational spring with rigid links joint model (scissors model) associated with the proposed backbone curve adequately represented the cyclic response of beam-column joint tests.

ACKNOWLEDGMENT

Financial assistance provided by U.S. National Science Foundation (NSF) award #0618804 through George E. Brown Jr. Network for Earthquake Engineering Simulation (NEES) and the Egyptian Department of Education award #2005292 through National Housing and Building Research Center is greatly appreciated.

REFERENCES

Alath, S., and Kunnath, S.K. (1995). Modeling Inelastic Shear Deformation in RC Beam-Column Joints. *Engineering Mechanics Proceedings of 10th Conference*, ASCE, New York, **Vol II**, 822-825.

ASCE/SEI 41/06. Seismic Rehabilitation of Existing Buildings. American Society of Civil Engineers. Virginia, USA

Celik O. C., and Ellingwood, B. R. (2008). Modeling Beam-Column Joints in Fragility Assessment of Gravity Load Designed Reinforced Concrete Frames. Journal of Earthquake Engineering. **12:**357-381.

Hassan, W. M. (2011). Analytical and Experimental Assessment of Seismic Vulnerability of Beam-Column Joints without Transverse Reinforcement in Concrete Buildings. PhD Dissertation, University of California, Berkeley, California, USA.

Hassan, W. M., Park, S., Lopez, R., Mosalam, K. M., and Moehle, J. P. (2010). Seismic Response of Older-Type Reinforced Concrete Corner Joints. Proceedings, *9th U.S. National Conference and 10th Canadian Conference of Earthquake Engineering*, Toronto, Canada, paper No. 1616.

Kent, D. C., and Park, R. (1971). Flexural Members with Confined Concrete. Journal of the Structural Division, ASCE, **97:7**, 1969–1990.

Lowes, L. N. and Altoontash, A. (2003). Modeling Reinforced Concrete Beam-Column Joints Subjected to Cyclic Loading. ASCE Journal of Structural Engineering. **129:12**, 1686–1697.

Pantelides, C. P., Hansen, J., Nadauld, J., and Reaveley, L. D. (2002). Assessment of Reinforced Concrete Building Exterior Joints with Substandard Details. PEER 2002/18, Pacific Earthquake Engineering Research Center, University of California, Berkeley, USA.

Park, S. (2010). Experimental and Analytical Studies on Old Reinforced Concrete Buildings with Seismically Vulnerable Beam-Column Joints. PhD Dissertation, University of California, Berkeley, USA.

Uzumeri, S. M. (1977). Strength and Ductility of Cast-in-Place Beam Column Joints. Reinforced Concrete Structures in Seismic Zones, SP-53, Hawkins, N. M., ed., American Concrete Institute, Detroit, Michigan.

Wong, H. F. (2005). Shear Strength and Seismic Performance of Non-Seismically Designed Reinforced Concrete Beam-Column Joints", PhD Dissertation, The Hong Kong University of Science and Technology.